Journal of the European Ceramic Society 22 (2002) 2501–2509

www.elsevier.com/locate/jeurceramsoc

Assessment of the high temperature elastic and damping properties of silicon nitrides and carbides with the impulse excitation technique

Gert Roebben[a,*], Ren-Guan Duan[a], Diletta Sciti[b], Omer Van der Biest[a]

[a]*Department of Metallurgy and Materials Engineering, K.U.Leuven, Kasteelpark Arenberg 44, B-3001 Heverlee, Belgium*
[b]*CNR-IRTEC, Research Institute for Ceramics Technology, via Granarolo 64, I-48018 Faenza, RA, Italy*

Received 7 October 2001; received in revised form 5 April 2002; accepted 14 April 2002

Abstract

The impulse excitation technique (IET), based on resonant vibration analysis, was used to determine the high temperature elastic and damping properties of hot-pressed silicon nitride (Si_3N_4) and silicon carbide (SiC) materials with Al- and Y-additives. The Si_3N_4 materials were doped with 2 wt.% of TiN to suppress the crystallization of intergranular glassy pockets. Near 1000 °C the investigated materials display a characteristic damping peak, which is essentially unaffected by temperature excursions up to 1400 °C. Two existing models which aim at linking elastic and damping properties with microstructural and micromechanical details, are considered. One of the models is used to provide an estimate of the amount of amorphous intergranular pocket phase. This type of information is of particular relevance since the high temperature deformation resistance of silicon based ceramics is severely dependent on the presence and amount of amorphous multiple grain pockets.

Keywords: Grain boundaries; Mechanical properties; Mechanical spectroscopy; SiC; Si_3N_4

1. Introduction

Sintered Si_3N_4 and SiC are candidate materials for load-bearing and wear-resistant components in, for example engines and heat exchangers. Si_3N_4 and SiC powder compacts are difficult to densify without additives, because of the covalent nature of the Si–C and Si–N bonds and the associated low self-diffusion coefficient. One route to obtain fully dense Si_3N_4 and SiC ceramics is liquid-phase sintering (LPS),[1–6] a method based on the addition of metal oxides to form a liquid phase during sintering. However, properties of LPS-ceramics are strongly affected by the intergranular residue of the liquid sintering medium, which can be (at least partially) glassy. At high temperatures, glass softens, thus drastically decreasing strength as well as oxidation and creep resistance. In order to limit these effects, 'exotic' sintering additives (Lu, Yb,...) are used to obtain a more refractory glass phase than the originally used Mg or Y, Al-additive systems.[7] One has also aimed at obtaining particular intergranular glass compositions, which are susceptible to crystallisation into a refractory phase upon annealing.[8] Another effect of annealing treatments is the modification of the grain boundary phase, such as its partial elimination due to the movement of liquid phase towards the sample surface and evaporation in the atmosphere.[1,2,5] Nevertheless, the majority of silicon-based LPS ceramics contains a residual amorphous phase.

With respect to the characterisation of the deformation behaviour of sintered ceramics at elevated temperature, mechanical spectroscopy (a set of techniques in which an oscillating mechanical stress interacts with a solid, leading to measurable internal friction, damping or energy losses[9]), has proven to be a valuable technique. Mosher, Raj and Kossowsky[10] were the first to use internal friction measurements to assess the grain boundary sliding resistance in Si_3N_4. The link between grain-boundary sliding and high temperature internal friction has been further established for fine-grained, sintered ceramics. The findings of Kleebe and Pezzotti[11] and Schaller[12] provide particular insight into the observations and will be used in the discussion of our results.

In this work, liquid-phase sintered silicon-based ceramics were characterised with respect to the change with temperature of the Young's modulus and internal fric-

* Corresponding author. Tel.: +32-16-321-192; fax: +32-16-321-992.
E-mail address: gert.roebben@mtm.kuleuven.ac.be (G. Roebben).

0955-2219/02/$ - see front matter
PII: S0955-2219(02)00111-5

tion up to 1400 °C. The applied method is a resonance vibration based analysis. The resonant frequencies (f_r) of a solid object are related to its mass, dimensions and elastic properties. For monolithic, isotropic samples of simple geometry one can calculate the elastic moduli of the test material from f_r. The internal friction, Q^{-1}, can be deduced with resonant vibration techniques as well, since Q^{-1} is related to the amplitude decay of a free vibration. One type of resonant vibration devices relies on impulse excitation: a light, non-destructive impact is given to the specimen to induce its resonant vibration. This *impulse excitation technique* (IET) can be applied at high temperatures. The IET is now a fully recognised standard test method for the determination of dynamic moduli of materials. When using appropriate sample dimensions, IET can provide highly accurate and reproducible *E*-modulus and internal friction values up to elevated temperatures. From these results, one can deduce physical and microstructural parameters such as Debye Temperature,[13] amount of dissolved atoms in solid solutions[14] or porosity.[15] This paper aims at establishing links between IET-data and the microstructural features which determine the high temperature deformation resistance of LPS-ceramics.

When interpreting the results of mechanical spectroscopy tests at elevated temperature, a major concern is that of the microstructural stability of the test material. Changes of the microstructure during the tests will affect the internal friction and stiffness curves, and typically result in differences between heating and cooling curves. The SiC and Si_3N_4 materials discussed in this paper have been selected based on the observation of an essentially stable internal friction and stiffness behaviour at temperatures up to 1300 °C or more. This facilitates the interpretation of the observed internal friction features and changes of stiffness at elevated temperature. The tested SiC materials were prepared at IRTEC-Faenza (Italy), the Si_3N_4 materials were prepared at MTM-K.U.Leuven (Belgium).

2. Experimental procedure

2.1. Preparation and characterisation of the test materials

2.1.1. Silicon carbide

The starting powders used to produce dense liquid phase sintered SiC were β-SiC powder (Starck BF-12), Al_2O_3 (Baikalox CR30), and Y_2O_3 (HC-Starck). The SiO_2 content of the as received SiC-powder (1.5 wt %) was reduced in a thermal treatment to 0.9 wt %. Two compositions were prepared. The material labelled SC-Y4Al6 consists of as received SiC-powder, with 6 wt.% Al_2O_3 and 4 wt.% Y_2O_3 additives, a ratio which corresponds to the lowest eutectic (1780 °C) in the Al_2O_3–Y_2O_3 system. This powder mixture contains about 1.4 wt.% SiO_2. The material labelled SC-Y4Al3 is made of a mixture of thermally treated SiC-powder with 2.7 wt.% Al_2O_3 and 3.5 wt.% Y_2O_3 additives, containing about 0.8 wt.% SiO_2. The selected Al_2O_3/Y_2O_3 ratio corresponds with the stoichiometry of the YAG phase ($3Y_2O_3.5Al_2O_3$). Densification was achieved through hot pressing at 1880 °C, under an applied pressure of 30 MPa, for 20–40 min. Annealing treatments were conducted in a graphite resistance furnace at 1900 °C for 3 h under an atmosphere of argon. After hot pressing the samples reached densities higher than 98.5% of theoretical density. The crystalline phases revealed by X-ray diffraction are mainly β-SiC, YAG, and traces of the α-SiC 6H and 4H polytypes already present in the starting powders; the β→α-SiC transition did not occur. Grain morphology is equiaxed with grain size distribution ranging from 0.1 to 2 μm, except for a small number of larger grains (up to 10 μm) with irregular shape. Plasma-etching reveals that adjacent SiC grains are separated by a thin grain boundary film. Volume-wise, the major part of the intergranular phases appears at three- and four-grain channels and pockets. During the annealing treatments at 1900 °C, the materials underwent weight losses of about 3% (SC-Y4Al3) and 5.5% (SC-Y4Al6), corresponding to carbo-thermal reduction and the resulting formation of volatile components as Al_2O, SiO and CO. Density decreased as a result of pore creation, originating from microstructure rearrangement. X-ray diffractograms showed that after thermal treatment, there was an evident reduction of crystalline YAG peaks. α-SiC 6H and 4H polytypes peaks were enhanced, indicating that the thermal treatments gave rise to the β→α-SiC transition. More details are reported in previous papers.[4,5,16]

2.1.2. Silicon nitride

The starting powders used are Si_3N_4 (HCST grade LC12-SX, 97% α-Si_3N_4, submicron particle size, 1.8–2.1 wt.% oxygen), Al_2O_3 (Baikowski grade SM8, 95% α, submicron particle size), TiN (Ceramyg, France, submicron particle size), and Y_2O_3 (Aldrich Chemical Company, 99.99% pure). Powder mixtures were prepared by alumina ball-milling in an alumina vessel (Retsch B.V., the Netherlands) for 4 h in isopropanol. The Al_2O_3 pick-up during ball milling was assessed by XRF (Philips, PW2400 X-ray Spectrometer, the Netherlands), using a calibration curve based on powder mixtures of Al_2O_3 and α-Si_3N_4. Different amounts of Al_2O_3 pick-up originate from different rotation speeds during ball milling. The nominal composition of the powder mixtures including the Al_2O_3 pick-up from ball milling is listed in Table 1. The major difference between the two prepared grades is the amount of Al_2O_3 (4 wt.% for SNY2Al4Ti2 and 3 wt.% for SNY2Al3Ti2).

Table 1
Composition of the powder mixtures (wt.%) including Al_2O_3 pick-up from ball milling

	SC-Y4Al6	SC-Y4Al3	SN-Y2Al4Ti2	SN-Y2Al3Ti2
SiC or Si_3N_4	90	93.8	91.5	93
Y_2O_3	4.0	3.5	2	2
TiN	0	0	2	2
Al_2O_3	6.0	2.7	4	0
Al_2O_3[a]	0	0	0.5	3.0

[a] The amount of Al_2O_3 pick-up during alumina ball milling.

Samples were hot pressed under vacuum (0.1 Pa) at 1650 °C for 1 h under a mechanical load of 20 MPa.

Scanning electron microscopy observations in combination with X-ray diffraction analysis enabled the identification of the constituent phases. Both grades contain α-sialon, β-sialon, TiN and O-sialon (=Al-substituted Si_2N_2O). High-temperature X-ray diffraction revealed that α-sialon, β-sialon and TiN phases are stable up to 1400 °C. The O-sialon phase has disappeared from the XRD-spectra taken at 1400 °C. More details have been reported previously[17] and are discussed in a companion paper.[18]

2.2. The impulse excitation technique (IET) to measure Young's modulus and internal friction

Rectangular beam-like samples cut from the hot-pressed disks were suspended in the nodes of their first bending vibration mode with carbon threads, and positioned in a IET-furnace (HTVP-1750-C, IMCE, Diepenbeek, Belgium). The furnace with graphite heating elements is three times evacuated and filled with dry N_2 (with 10 ppm H_2O) before heating. The sample subsequently is subjected to two thermal cycles from 100 to 1400 °C with a heating and cooling rate of 2 °C/min. The sample is excited periodically by the impact of a small ceramic projectile.[19] The vibration signal, captured by a microphone, was analysed with the Resonance Frequency and Damping Analyser (RFDA, IMCE, Diepenbeek, Belgium). As described elsewhere in detail,[19] the RFDA performs a Fourier transformation of the digitised acoustic signal, thus providing starting values for an iterative algorithm, in which the acoustic signal is simulated as a sum of exponentially damped sinusoidal vibrations. For linear anelastic materials, with an amplitude-independent behaviour, the simulation results in a set of accurately determined resonance frequencies and the corresponding exponential loss factors. At low stress amplitudes, amplitude independent behaviour is generally observed for dense ceramics, as has been verified for a liquid phase sintered Si_3N_4.[20]

In the particular case of the bars suspended in the furnace, the spectrum contained only one major frequency. From this flexural vibration frequency f_b the E-modulus was calculated according to the equation proposed in ASTM E 1876–97[21] and ENV 843–2:[22] $E = 0.9465(m(f_b)2/b)(L^3/t^3)T_1$, with m, L, b and t, the sample weight, length, width, and thickness, respectively. T_1 is a correction factor, depending on the Poisson's ratio and the thickness/length ratio. Some of the samples had a length/width ratio of about 4. The resulting plate-like rather than beam-like vibration behaviour was corrected for using an extra correction factor.[16] When performing high temperature IET-tests, the effect of thermal expansion on the sample dimensions must be accounted for. The correction formula proposed in ASTM 1876-97[21] was used, assuming a constant thermal expansion coefficient of 4.6×10^{-6}/K for SiC and 3.4×10^{-6}/K for Si_3N_4.[23] Neglecting this correction would induce an overestimation of the E-modulus by about 0.5% at 1400 °C. The internal friction corresponding to the flexural vibration mode is calculated as $Q^{-1} = k/(\pi f_b)$, where k is the exponential decay parameter of the amplitude of the flexural vibration component.

3. Impulse excitation test results

The changes of stiffness and internal friction of the SiC and Si_3N_4 samples are strongly similar, as is shown in Fig. 1. In this graph two of the tested materials are compared, i.e. SC-Y4Al6 (SiC with 6 wt.% Al_2O_3 and 4 wt.% Y_2O_3, as hot-pressed) and SN-Y2Al4Ti2 (Si_3N_4 with 2 wt.% Y_2O_3, 4 wt.% Al_2O_3 and 2 wt.% TiN). The comparison of the two materials is facilitated by the fact that both samples have a bending resonance frequency of 12 kHz, and by using the relative change of the E-modulus rather than the absolute values.

When increasing the temperature from room temperature, the stiffness decreases slowly at a rate of 21

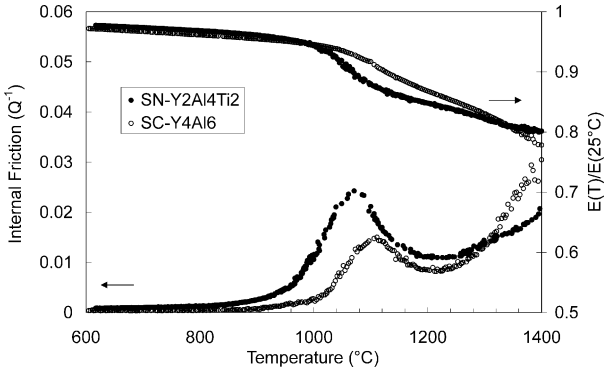

Fig. 1. Comparison of the stiffness and internal friction curves of a hot-pressed SiC (SC-Y4Al6, $f_b = 12$ kHz) and a hot-pressed Si_3N_4 (SN-Y2Al4Ti2, $f_b = 12$ kHz).

MPa/°C for SiC, and at 12 MPa/°C for Si_3N_4. At a material-specific temperature the stiffness decrease accelerates, and the internal friction rises. The steepest stiffness decrease coincides with an internal friction peak, which is higher for SN-Y2Al4Ti2 than for SC-Y4Al6. Internal friction and the rate of stiffness loss increase again at more elevated temperatures. At about 1300–1325 °C the stiffness and internal friction curves of SN-Y2Al4Ti2 and SC-Y4Al6 cross over. This indicates that the rate of the increase of internal friction at high-temperature is not solely determined by the size of the Q^{-1}-peak.

Fig. 2 illustrates a common observation for the materials reported on in this paper, i.e. the essentially unchanged aspect of internal friction and stiffness curves when comparing heating and cooling stages. This observation is illustrated with the results of the SN-Y2Al4Ti2 sample. This is not a common observation for LPS-Si_3N_4 ceramics. Most often the internal friction peak is either reduced or eliminated after elevated temperature tests.[24–26] In the case of the SN-Y2Al3Ti2 and SN-Y2Al4Ti2 materials, only a small but steadily proceeding shift of the internal friction background can be discerned over several heating cycles. This is possibly linked to the instability of the O-sialon phase in the presence of an amorphous intergranular phase at temperatures above 1300 °C as observed with high temperature XRD.[18]

Stiffness and internal friction in the neighbourhood of the internal friction peaks for both SiC and both Si_3N_4 materials are shown in respectively Figs. 3 and 4. The materials with a higher amount of sintering additives have a more pronounced change of stiffness and a larger internal friction peak than the materials containing less sintering additives. With respect to the SiC materials, the comparison reveals that the internal friction peak has disappeared after the 3 h annealing heat treatment at 1900 °C in Argon.

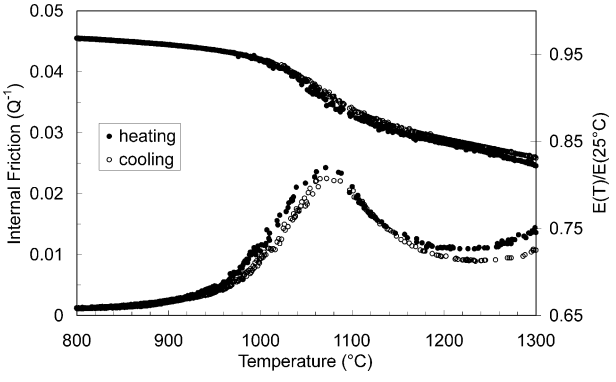

Fig. 2. Internal friction and stiffness of SN-Y2Al4Ti2 during heating and successive cooling.

4. Discussion

4.1. The internal friction peak near 1100 °C

The impulse excitation tests revealed the presence of a Q^{-1}-peak in the as-hot-pressed SiC and Si_3N_4 materials. In this respect, the IET-results strongly resemble the results of mechanical spectroscopy tests performed earlier on liquid phase sintered silicon nitride materials, after the original work of Mosher, Raj and Kossowsky.[10] In the last decade, two research teams have provided the majority of mechanical spectroscopy results on non-oxide polycrystalline ceramics at high temperature. Both Pezzotti et al.[11,25] and Schaller et al.[12,26] have proposed micromechanical models explaining the origin of the characteristic internal friction peaks in their observations. Their findings are briefly compared in another paper[16] and more extensively in the dissertation of Roebben.[27] In this paper both interpretations are applied to the reported stiffness and damping data, to provide a micromechanical interpretation of the differences observed between the tested materials.

An important observation is that, after the IET-tests up to 1400 °C, the shape and position of the Q^{-1}-peak remain essentially unaffected. This excludes the interpretation of the peak as a transitory irreversible effect associated with, for example, crystallisation. Instead, relaxation effects, which do not alter the microstructure, such as proposed by Pezzotti et al. (grain boundary sliding) and Schaller et al. (softening of amorphous pockets in a rigid ceramic skeleton) can be considered.

4.1.1. Estimation of the intrinsic grain boundary viscosity

Assuming the peak is due to grain boundary sliding, and applying the procedure proposed by Pezzotti et al.[28] it is possible to deduce an estimate for the intrinsic grain boundary viscosity at the peak temperature from the Q^{-1}-peak frequency. The calculation requires the knowledge of several microstructural and mechanical parameters. Two equations are involved. Eq. (1), first proposed by Mosher and Raj,[29] relates the intrinsic grain boundary viscosity η to the frequency at the peak temperature, f_{peak}:

$$\eta = \frac{G_{LT}\delta}{2\pi f_{peak}\alpha(1-\nu)d} \tag{1}$$

This equation involves G_{LT}, the unrelaxed shear modulus, i.e. the shear modulus at the low-temperature foot of the Q^{-1}-peak. δ is the grain boundary film thickness, ν is the Poisson's ratio, d the grain size, and α a grain morphology parameter. Pezzotti proposed to deduce α from the ratio of the unrelaxed G-modulus and the shear modulus G_{peak} at the Q^{-1}-peak-temperature [Eq. (2)].[28]

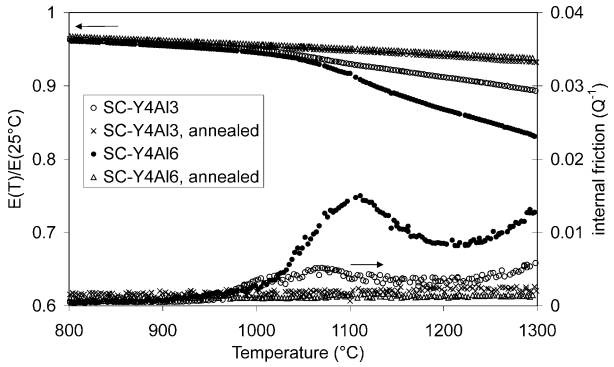

Fig. 3. Stiffness and internal friction in SC-Y4Al3 and SC-Y4Al6, as-hot-pressed and after annealing at 1900 °C.

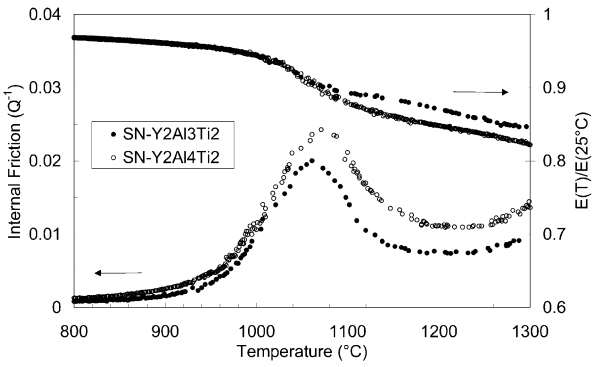

Fig. 4. Comparison of stiffness and internal friction of SN-Y2Al3Ti2 and SN-Y2Al4Ti2.

$$\alpha = \frac{\frac{G_{LT}}{G_{peak}} - 1}{1 - \nu} \quad (2)$$

The characteristics of the peaks and the microstructural and mechanical properties required to calculate η for SN-Y2Al3Ti2, SN-Y2Al4Ti2, SC-Y4Al3 and SC-Y4Al6 are summarised in Table 2. In our calculations we have assumed that the shear modulus G and the Young's modulus E change with temperature in a similar manner. The grain boundary film thickness is estimated at 1 nm, a value typical for liquid-phase sintered ceramics. The effect of a change of δ, say between 0.5 and 1.5 nm, will slightly affect the calculated viscosity, but not its order of magnitude. The mean grain size of the SiC ceramics was carefully determined through a linear intercept method on micrographs of plasma-etched surfaces.[5] The grain size of the Si_3N_4 materials was estimated from SEM-micrographs.

The viscosity values obtained are 1.0×10^5 Pa s for SC-Y4Al6 at 1112 °C and 1.8×10^5 Pa s for SC-Y4Al3 at 1085 °C. These values are considerably lower than the viscosity of the intergranular silicate phase in 2.65 mol% BaO-doped SiC at this temperature (10^9 Pa s at 1100 °C[30]). For the Si_3N_4 samples, viscosity values of 1.8×10^4 Pa s (SN-Y2Al3Ti2 at 1061 °C) and 3.1 10^4 Pa.s (SN-Y2Al4Ti2 at 1065 °C) are obtained. These estimates are also rather low in comparison to the reported viscosity values of YSiAlON glass materials (10^8 Pa s at 1100 °C,[31] 5×10^6 Pa s at 1100 °C[32]) or SiAlON intergranular glass phases.[33]

4.1.2. Estimation of the volume fraction of intergranular amorphous pockets

The Q^{-1}-peak can also be interpreted according to the approach of Schaller et al.[12,24] which links the Q^{-1}-peak to the glass transition of amorphous pockets in a rigid ceramic skeleton. When the amorphous pocket phases in LPS-ceramics go through their glass transition, the

Table 2
Microstructural parameters, mechanical properties and IET-data used for the micromechanical calculations, and the results of the latter

Property	Unit	SC-Y4Al6	SC-Y4Al3	SN-Y2Al3Ti2	SN-Y2Al4Ti2
Poisson's ratio, ν	–	0.2	0.2	0.28	0.28
Intergranular film thickness, δ	nm	1[a]	1[a]	1[a]	1[a]
Grain size, d	μm	0.54	0.63	0.75[a]	0.75[a]
Temperature at lower foot of Q^{-1}-peak, T_{LT}	°C	900	900	850	850
E-modulus at T_{LT}, E_{LT}	GPa	372.4	416.1	283.0	289.4
E_{LT} corrected for decay of E with temperature below T_{LT}, E_{LC}	GPa	368	412	280	286.9
Shear modulus at T_{LT}	GPa	155	173	111	113
Temperature of Q^{-1}-peak, T_{peak}	°C	1112	1085	1061	1070
Resonance frequency at T_{peak}	Hz	11304	11430	22005	11460
E-modulus at T_{peak}, E_{peak}	GPa	358	407.5	267	271.3
E_{peak}/E_{LT}	–	0.961	0.979	0.943	0.937
Temperature at higher foot of Q^{-1}-peak, T_{HT}	°C	1221	1191	1157	1169
E-modulus at T_{HT}, E_{HT}	GPa	340.0	399.8	258.8	257.1
E_{HT} corrected for decay of E with temperature above T_{HT}, E_{HC}	GPa	350	407	265	264
Estimated value of the E-modulus of the glass pockets at T_{LT}	GPa	120[a]	120[a]	120[a]	120[a]
Calculated grain boundary film viscosity, η	Pa s	1.0×10^5	1.8×10^5	1.8×10^4	3.1×10^4
Calculated volume fraction of amorphous pocket phase, V_p	vol.%	5.8	2.2	5.0	7.3

[a] Estimated values.

viscosity evolves from too high to deform to too low to dissipate energy. In between the viscosity reaches a level corresponding with maximum energy dissipating capacity under cyclic loading. If the peak is due to gradual melting of residual amorphous pockets, one can relate the volume fraction of amorphous pockets with the loss of stiffness associated with the Q^{-1}-peak in the following manner.

At temperatures beneath the Q^{-1}-peak, the material is considered as a particulate composite, with a SiC or Si_3N_4 matrix and solid, linear-elastic glassy inclusions. The stiffness of a material consisting of two solid phases is related to the stiffness of the individual phases and their volume fraction. Upper and lower boundary values for the composite stiffness can be determined from Voigt and Reuss approximations, an approach followed by Besson et al. who investigated the crystallisation kinetics of YSiAlON glass ceramics.[34] A more narrow yet accurate set of boundary values is provided by Ravichandran.[35] In terms of the particular case studied here, his analytical equations estimate the stiffness of the composite at the low-temperature foot of the Q^{-1}-peak (E_{LT}) as follows:

Lower boundary:

$$E_{LT} = \frac{\left[\left(cE_{pocket}E_{matrix} + E_{matrix}^2\right)(1+c)^2 - E_{matrix}^2 + E_{pocket}E_{matrix}\right]}{\left(cE_{pocket} + E_{matrix}\right)(1+c)^2} \tag{3}$$

Upper boundary:

$$E_{LT} = \frac{\left[E_{pocket}E_{matrix} + E_{matrix}^2(1+c)^2 - E_{matrix}^2\right](1+c)}{\left(E_{pocket} - E_{matrix}\right)c + E_{matrix}(1+c)^3} \tag{4}$$

In these equations, c is a non-dimensional parameter related to the volume fraction V_{pocket} of the pocket phase:

$$c = \sqrt[3]{\frac{1}{V_{pocket}}} - 1 \tag{5}$$

Hence, upper and lower boundary values for E_{LT} can be calculated from the volume fraction of the pockets, V_{pocket}, the stiffness of the matrix material, E_{matrix}, and the stiffness of the pockets, E_{pocket}. At temperatures above the high-temperature foot of the Q^{-1}-peak, the glass pockets have a very low stiffness and can be tentatively approximated as pores. In this case, the relation between the stiffness at the high-temperature foot of the Q^{-1}-peak (E_{HT}) and the volume fraction of pockets is given by Eq. (6)[36]

$$E_{HT} = E_{matrix}\left(1 - 1.9V_{pocket} + 0.9\left(V_{pocket}\right)^2\right) \tag{6}$$

One can combine Eq. (3) or (4) with Eq. (6) to eliminate E_{matrix}. However, between the lower and the higher temperature foot of the internal friction peak, E_{matrix} changes. Therefore, the values of E_{HT} and E_{LT} are corrected for the decay of stiffness with temperature. The correction of E_{LT} is based on the slope of the E vs. T curve at temperatures below the internal friction peak, the correction of E_{HT} on the slope after this peak. Substituting the measured and corrected values of E_{LT} and E_{HT}, one obtains an equation with V_{pocket} and E_{pocket} as the only variables.

It was chosen to estimate the E-modulus of the glass phase in the pockets, leaving an equation with only V_{pocket} as a variable. A review of reported E-modulus values of Y–Si–Al–O–N and Y–Si–Al–O–C revealed a high consistency between individual results, allowing estimating E_{pocket} at 120 ± 10 GPa for both SiC and Si_3N_4 materials. [34,37–40] Calculations were made using the data presented in Table 2. The lower and upper estimates of the amount of glassy pockets are obtained through a graphic analysis of the equations. The 10 GPa estimation error on the value of E_{pocket} corresponds with less than 1 vol.% error on the calculated estimates for V_{pocket}.

The simple arithmetic average was selected for averaging upper and lower bounds.[36] This leads to estimates of V_{pocket} of 5.8 vol.% for SC-Y4Al6 and 2.2 vol.% for SC-Y4Al3. Compared with the SiO_2-content of the starting powders (SC-Y4Al6 contains 1.4 wt.% and SC-Y4Al3 contains 0.8 wt.%), and bearing in mind the presence of the thin amorphous intergranular film, the calculated V_{pocket} values are rather large. However, undoubtedly part of the Al_2O_3 and Y_2O_3 additives have entered the intergranular glass structure. The results for the Si_3N_4 samples show a similar trend. The sample sintered with more additives (SN-Y2Al4Ti2) has a higher V_{pocket} value (7.3%) than SN-Y2Al3Ti2 (5.0%).

4.1.3. Remarks

The above calculations aimed at providing a quantitative link between the Q^{-1}-peak and the associated stiffness relaxation on the one hand, and the grain-boundary viscosity or the volume fraction of amorphous pockets, on the other hand. Notwithstanding the approximations made in some of the required microstructural and micromechanical parameters, and unlike the obtained grain boundary viscosity values, the estimated V_{pocket} values are realistic. This indicates that the Q^{-1}-peaks observed in the as-hot-pressed SiC and Si_3N_4 materials discussed in this paper are due to the presence and softening of glassy pockets.

The methodology presented above to estimate the amount of amorphous intergranular phase is interesting, since—to the author's knowledge—there is no existing workable alternative. SEM image analysis methods lack the information about the crystallinity of

the intergranular phase. TEM-image analysis does allow distinguishing amorphous and crystalline pockets, but lacks the statistical reliability and averaging capacity offered by the mechanical spectroscopy results. The proposed method may be developed further to take into account the diverse geometry of the glassy intergranular phase, as it is present not only as isolated pockets, but also as interconnected three-grain-junction channels.

Whereas X-ray diffraction already indicated the decrease of the amount of crystalline YAG as intergranular phase after the annealing treatment at 1900 °C, the disappearance of the Q^{-1}-peak additionally demonstrates that the annealing treatment effectively reduces the amount of amorphous intergranular pockets. Actually, the residual amount of glass pockets after annealing at 1900 °C for 3 h is below the IET-detection limit, suggesting that the effect of any remaining glass pockets on the macro-mechanical properties can be neglected.

4.2. The exponential damping background

A second feature in the IET-observations is the damping 'background' at elevated temperature. Rather than considering the Q^{-1}-peak at 1100 °C as the anelastic grain boundary sliding peak, one can interpret the exponential background as the low-temperature foot of a grain boundary sliding peak at more elevated temperature. In that case, the observed decrease of the exponential background upon annealing corresponds to the shift of this grain-boundary-sliding peak to an even more elevated temperature, and/or to a substantial reduction of the peak height. In any case, this would mean that the anelastic grain-boundary-sliding mechanism has become more difficult after annealing. The lower damping at high temperatures can also be looked upon as the decrease of the exponential background as such. In this case, the conclusion is that the resistance of the LPS-SiC to viscoplastic creep deformation has increased after annealing.[12] Even if the presented IET-results do not allow distinguishing between the anelastic and viscoplastic interpretations, they necessarily lead to the conclusion that the grain boundary sliding resistance has increased considerably after the annealing treatment.

The observed increase of the grain boundary sliding resistance of the SiC materials after annealing is at least partially explained by the disappearance of the amorphous pockets, which constitute reservoirs of viscous material to enhance processes of viscous flow and grain boundary sliding. However, other microstructural parameters (grain size, grain boundary film thickness, composition and therefore viscosity, ...) play a role as well. Only this can explain why the damping background of the SiC materials increases more rapidly with temperature than the damping background of the Si_3N_4 materials (Fig. 1) even if the latter have a larger V_{pocket}. With respect to the annealing treatments on the SiC materials, it is suspected that also the grain boundary film itself has become more sliding resistant. However, only HR-TEM can convincingly reveal and distinguish a decreased intergranular film thickness and/or a change of its chemistry towards a more pure SiO_2-composition, both of which are known to increase the grain boundary sliding resistance.[11,24]

4.3. Particular assets of the impulse excitation technique

The above observations are of particular relevance for the use of liquid phase sintered ceramics at elevated temperatures and demonstrate one of the assets of the IET: a rapid and non-destructive assessment of the small-amplitude deformation resistance. In addition, it can be noticed that, also with respect to other mechanical spectroscopy tests, IET provides the possibility to test components, and not only test samples of simple rectangular shape.[41] Hence, since it was observed that the IET-test itself does not affect the integrity of the sample, the technique can be further developed as a highly informative non-destructive quality control test. As such, the IET-equipment used is the only apparatus that provides accurate high temperature damping measurements on ceramic components. Its results can be compared with the more fundamental insights provided by, for example, torsion pendulum tests, and complementary techniques to characterise the grain boundary sliding resistance such as the more time-consuming creep study. The latter provides important information about rupture and lifetime.[7,42]

5. Conclusions

In this paper the results of non-destructive impulse excitation tests were used to study the high temperature elastic and damping behaviour of liquid phase sintered Si_3N_4 and SiC materials. In particular, the IET test results were compared with established interpretations of the high temperature damping characteristics of liquid phase sintered ceramics. A method is proposed to estimate the amount of intergranular amorphous pockets. It was shown that a 3 h heat treatment of the SiC materials at 1900 °C in argon effectively eliminates the amorphous intergranular pockets.

Acknowledgements

G. Roebben thanks the Fund for Scientific Research (FWO)—Vlaanderen for his research fellowship. R.G. Duan thanks the academic board of the Katholieke Universiteit Leuven for a Junior Fellowship.

References

1. Dressler, W. and Riedel, R., Progress in silicon-based non-oxide structural ceramics. *Int. J. Refractory Metals and Hard Materials*, 1997, **15**, 13–47.
2. Van Dijen, F. K. and Mayer, E., Liquid phase sintering of silicon carbide. *J. Eur. Ceram Soc*., 1996, **16**, 413–420.
3. Falk, L. K., Microstructural development during liquid phase sintering of silicon carbide ceramics. *J. Eur. Ceram. Soc*., 1997, **17**, 983–994.
4. Sciti, D. and Bellosi, A., Effect of additives on densification, microstructure and properties of liquid- phase sintered silicon carbide. *J. Mat. Sci*., 2000, **35**, 3849–3855.
5. Sciti, D., Guicciardi, S. and Bellosi, A., Effect of annealing treatments on microstructure and mechanical properties of liquid-phase sintered silicon carbide. *J. Eur. Ceram. Soc*., 2001, **21**, 621–632.
6. Sigl, L. S. and Kleebe, H.-J., Core/rim structure of liquid-phase-sintered silicon carbide. *J. Am. Ceram. Soc*., 1993, **76**, 773–776.
7. Lofaj, F., Wiederhorn, S. M., Long, G. G., Jemian, P. R. and Ferber, M. K., Cavitation creep in the next generation silicon nitride. In *Proceedings of the 7th International Symposium Ceramic Materials and Components for Engines*, ed. J. G. Heinrich and F. Aldinger. Wiley-VCH Verlag, Weinheim, Germany, 2001, pp. 487–493.
8. Lewis, M. H. and Lumby, R. J., Nitrogen ceramics: liquid phase sintering. *Powder Metallurgy*, 1983, **26**, 73–81.
9. Schaller, R., Fantozzi, G., Gremaud, G., ed., *Mechanical Spectroscopy Q^{-1} 2001, Materials Science Forum Vols. 366–368*. Trans Tech Publications, Zürich, Switzerland, 2001.
10. Mosher, D. R., Raj, R. and Kossowsky, R., Measurement of viscosity of the grain-boundary phase in hot-pressed silicon nitride. *J. Mater. Sci*., 1976, **11**, 49–53.
11. Kleebe, H.-J. and Pezzotti, G., Transmission electron microscopy in conjunction with internal friction measurements—a powerful tool for characterization of ceramic interfaces. *J. Ceram. Soc. Japan*, 1999, **107**, 801–813.
12. Schaller, R., Mechanical spectroscopy of the high temperature brittle-to-ductile transition in ceramics and cermets. *J. Alloys Comp*., 2000, **310**, 7–15.
13. Bruls, R. J., Hintzen, H. T., de With, G. and Metselaar, R., The temperature dependence of the Young's modulus of $MgSiN_2$, AlN and Si_3N_4. *J. Eur. Ceram. Soc*., 2001, **21**, 263–268.
14. Weller, M., Point defect relaxations. In *Mechanical Spectroscopy Q^{-1} 2001, Materials Science Forum Vols. 366–368*, ed. R. Schaller, G. Fantozzi and G. Gremaud. Trans Tech Publications, Zürich, Switzerland, 2001, pp. 95–140.
15. Panteliou, S. D. and Dimarogonas, A. D., Thermodynamic damping in porous materials with spherical cavities. *Shock and Vibration*, 1997, **4**, 261–268.
16. Roebben, G., Sciti, D., Lauwagie, T., Bellosi, A., Van der Biest, O., High temperature stiffness and damping measurements to monitor the glassy intergranular phase in liquid-phase-sintered silicon carbide. *J. Am. Ceram. Soc*. (submitted for publication).
17. Duan, R.G., Roebben, G., Vleugels, J., Van der Biest, O., Stability of intergranular phases in hot pressed Si_3N_4 studied with mechanical spectroscopy and in-situ high-temperature XRD. *J. Eur. Ceram. Soc*., 2002, **22**, 1897–1904.
18. Duan, R. G., Roebben, G., Vleugels, J., Van der Biest, O., Thermal stability of in-situ formed Si_3N_4-Si_2N_2O-TiN composites. *J. Eur. Ceram. Soc*., 2002, **22**, 2527–2535.
19. Roebben, G., Bollen, B., Brebels, A., Van Humbeeck, J. and Van der Biest, O., Impulse excitation apparatus to measure resonant frequencies, elastic moduli, and internal friction at room and high temperature. *Rev. Sci. Instrum*., 1997, **68**, 4511–4515.
20. Roebben, G., Donzel, L., Sakaguchi, S., Steen, M., Schaller, R. and Van der Biest, O., Internal friction under low-amplitude torsional and high-amplitude uniaxial load in silicon nitride. *Scripta Mater*., 1997, **36**, 165–171.
21. *Standard test method for dynamic Young's modulus, shear modulus, and Poisson's ratio by impulse excitation of vibration*, E 1876–97, American Society for Testing and Materials, West Conshohocken, PA (1998).
22. *Advanced technical ceramics—Monolithic ceramics, mechanical properties at room temperature—Part 2: Determination of elastic moduli*, ENV 843–2, European Committee for Standardisation, Brussels (1995).
23. Roebben, G., Zhao, C., Duan, R. G., Vleugels, J., Heyns, M. and Van der Biest, O., In-situ high temperature study of ceramics and ceramic ultra-thin films using a X-ray diffractometer with a parabolic multilayer mirror. *Key Engineering Materials*, 2002, **206–213**, 775–778.
24. Roebben, G., Donzel, L., Stemmer, S., Steen, M., Schaller, R. and Van der Biest, O., Viscous energy dissipation in silicon nitride at high temperatures. *Acta Mater*., 1998, **46**, 4711–4723.
25. Ota, K. and Pezzotti, G., Internal friction study of sialon ceramics. *Phil. Mag. A*, 1996, **73**, 223–235.
26. Lakki, A., Schaller, R., Bernard-Granger, G. and Duclos, R., High temperature anelastic behaviour of silicon nitride studied by mechanical spectroscopy. *Acta Metall. Mater*., 1995, **43**, 419–426.
27. Roebben, G., Viscous Energy Dissipation in Silicon Nitride at High Temperature. PhD thesis, K.U.Leuven, Belgium, 1999.
28. Pezzotti, G., Ota, K. and Kleebe, H.-J., Grain-boundary relaxation in high-purity silicon nitride. *J. Am. Ceram. Soc*., 1996, **79**, 2237–2246.
29. Mosher, D. R. and Raj, R., Use of the internal friction technique to measure rates of grain boundary sliding. *Acta Metall*., 1974, **22**, 1469–1474.
30. Pezzotti, G., Nishimura, H., Ota, K. and Kleebe, H.-J., Grain-boundary viscosity of BaO-doped SiC. *J. Am. Ceram. Soc*., 2000, **83**, 563–570.
31. Rouxel, T. and Verdier, P., SiC particle reinforced oxynitride glass and glass-ceramic composites: crystallization and viscoplastic forming ranges. *Acta Mater*., 1996, **44**, 2217–2225.
32. Donzel, L., *Intra- and Intergranular High Temperature Mechanical Loss in Zirconia and Silicon Nitride*. PhD thesis, Ecole Polytechnique Fédérale de Lausanne, 1998.
33. Pezzotti, G., Kleebe, H.-J., Okamoto, K. and Ota, K., Structure and viscosity of grain boundary in high-purity SiAlON ceramics. *J. Am. Ceram. Soc*., 2000, **83**, 2549–2555.
34. Besson, J.-L., Lemercier, H., Rouxel, T. and Trolliard, G., Yttrium sialon glasses: nucleation and crystallization of $Y_{35}Si_{45}Al_{20}O_{83}N_{17}$. *J. Non-Crystalline Solids*, 1997, **211**, 1–21.
35. Ravichandran, K. S., Elastic properties of two-phase composites. *J. Am. Ceram. Soc*., 1994, **77**, 1178–1184.
36. Green, D. J., *An Introduction to the Mechanical Properties of Ceramics*. Cambridge Solid State Science Series, Cambridge University Press, 1998.
37. Ramesh, R., Chevaux, P., Lemercier, H., Pomeroy, M. J. and Hampshire, S., Characterization of oxycarbide glasses prepared by melt solidification. *Key Engineering Materials*, 1997, **132–136**, 189–192.
38. Rouxel, T., Sangleboeuf, J.-C., Verdier, P. and Laurent, Y., Elasticity, stress relaxation and creep in SiC reinforced oxynitride glass. *Key Engineering Materials*, 2000, **171–174**, 733–740.
39. Rouxel, T. and Buisson, M., Physics of the brittle-ductile transition in glasses and glass-containing ceramics: time and temperature incidences. *Key Engineering Materials*, 1999, **166**, 65–72.
40. Inaba, S., Todaka, S., Ohta, Y. and Morinaga, K., Equation for estimating the Young's modulus, shear modulus and Vickers hardness of aluminosilicate glasses. *J. Japan Inst. Metals*, 2000, **64**, 177–183.

41. Roebben, G., Duan, R. G., Basu, B., Vleugels, J. and Van der Biest, O., The impulse excitation technique for rapid assessment of the temperature dependence of structural properties of silicon nitride and zirconium oxide ceramics. In *Proceedings of the 7th International Symposium Ceramic Materials and Components for Engines*, ed. J. G. Heinrich and F. Aldinger. Wiley-VCH Verlag, Weinheim, Germany, 2001, pp. 217–222.
42. Jensen, R. P., Luecke, W. E., Padture, N. P. and Wiederhorn, S. M., High-temperature properties of liquid-phase-sintered α-SiC. *Mat. Sci. Eng. A*, 2000, **A282**, 109–114.